



Volumes 446–447

31 October 2007  
ISSN 0925-8388

# Journal of ALLOYS AND COMPOUNDS

An Interdisciplinary Journal  
of Materials Science and  
Solid-State Chemistry and Physics

EDITOR-IN-CHIEF  
K. H. J. BUSCHOW

EDITORS  
H. KLEINKE  
H.G. PAN  
H. SAKAGUCHI

Proceedings of the International Symposium on  
Metal–Hydrogen Systems, Fundamentals and  
Applications (MH2006)  
October 1–6, 2006, Lahaina, Maui Island, Hawaii, USA

Guest Editors: R.C. Bowman Jr.  
T.J. Udovic  
C.M. Jensen

This article was published in an Elsevier journal. The attached copy is furnished to the author for non-commercial research and education use, including for instruction at the author's institution, sharing with colleagues and providing to institution administration.

Other uses, including reproduction and distribution, or selling or licensing copies, or posting to personal, institutional or third party websites are prohibited.

In most cases authors are permitted to post their version of the article (e.g. in Word or Tex form) to their personal website or institutional repository. Authors requiring further information regarding Elsevier's archiving and manuscript policies are encouraged to visit:

<http://www.elsevier.com/copyright>



ELSEVIER

Journal of Alloys and Compounds 446–447 (2007) 484–488

---



---

 Journal of  
 ALLOYS  
 AND COMPOUNDS
 

---



---

www.elsevier.com/locate/jallcom

# Positron annihilation study of hydrogen trapping at open-volume defects: Comparison of nanocrystalline and epitaxial Nb thin films

J. Cizek<sup>a,\*</sup>, I. Prochazka<sup>a</sup>, S. Danis<sup>a</sup>, O. Melikhova<sup>a</sup>, M. Vlach<sup>a</sup>, N. Zaludova<sup>a</sup>, G. Brauer<sup>b</sup>,  
W. Anwand<sup>b</sup>, A. Mücklich<sup>b</sup>, R. Gemma<sup>c</sup>, E. Nikitin<sup>c</sup>, R. Kirchheim<sup>c</sup>, A. Pundt<sup>c</sup>

<sup>a</sup> Faculty of Mathematics and Physics, Charles University in Prague, V Holesovickach 2, CZ-18000 Praha 8, Czech Republic

<sup>b</sup> Institut für Ionenstrahlphysik und Materialforschung, Forschungszentrum Rossendorf, Postfach 510119, D-01314 Dresden, Germany

<sup>c</sup> Institut für Materialphysik, Universität Göttingen, Friedrich-Hund-Platz 1, D-37077 Göttingen, Germany

Received 27 September 2006; received in revised form 1 December 2006; accepted 26 December 2006

Available online 10 January 2007

## Abstract

H interaction with defects in thin Nb films was investigated in this work. Thin Nb films were prepared by the cold cathode beam sputtering. First, microstructure of the as deposited films was characterized. The films sputtered at room temperature exhibit nanocrystalline grains, while those sputtered at high temperature ( $T = 850\text{ °C}$ ) are epitaxial. Subsequently, the films were step-by-step electrochemically charged with H. Development of microstructure and evolution of defect structure with increasing H concentration was investigated by slow positron implantation spectroscopy combined with X-ray diffraction. It was found that H is trapped at open-volume defects in the thin films of both kinds. The nanocrystalline films exhibit significantly extended H solubility in the  $\alpha$ -phase. Formation of the hydride-phase (Nb-H) at higher H concentrations leads to introduction of new defects. These are most probably dislocation loops that are emitted by growing hydride-phase particles.

© 2007 Elsevier B.V. All rights reserved.

**Keywords:** Thin films; Metal hydrides; Point defects; Positron spectroscopies; X-ray diffraction

## 1. Introduction

The behavior of H in a host metal lattice can be significantly influenced by interaction with lattice defects [1]. Defect studies of H-loaded samples are, therefore, highly important for an understanding of H behavior in metals. Positron annihilation spectroscopy (PAS) is a well-developed non-destructive technique with a high sensitivity to open-volume defects [2] and represents an ideal tool for the investigations of H-defect interactions. The aim of the present work is to investigate microstructural changes in H-loaded thin Nb films. Defect studies of the films were performed by slow positron implantation spectroscopy (SPIS) with measurement of Doppler broadening (DB) of the annihilation line. The H-induced lattice expansion was detected by X-ray diffraction (XRD). The results of these techniques were combined with direct observations of the microstructure by transmission electron microscopy (TEM).

## 2. Experimental details

Thin Nb films were prepared by the cold cathode beam sputtering in an UHV chamber. The nanocrystalline films were sputtered at room temperature on polished (100) Si substrates, while the epitaxial films were sputtered at  $850\text{ °C}$  on polished (11 $\bar{2}$ 0) sapphire substrates. The surface of all samples was covered at room temperature with a 20 nm thick Pd cap in order to prevent oxidation and to facilitate H absorption. The thickness of the studied films was determined by profilometry and by TEM. It lies in the range 1100–1150 nm. The orientation relationship of the epitaxial film with respect to the sapphire substrate is such that the three-fold axes of the Nb and sapphire are aligned parallel, i.e.  $[\bar{1}11]_{\text{Nb}} \parallel [0001]_{\text{sapphire}}$  and the (110)<sub>Nb</sub> planes are parallel to the (11 $\bar{2}$ 0)<sub>sapphire</sub> planes. The samples were step-by-step loaded with H by electrochemical charging, see Ref. [1] for details. Defect studies were performed on a magnetically guided positron beam “SPONSOR” [3] with positron energy adjustable from 0.03 to 36 keV. The energy spectra of the annihilation  $\gamma$ -rays were measured by a Ge detector with an energy resolution of  $(1.09 \pm 0.01)\text{ keV}$  at 511 keV. The DB of the annihilation peak was quantified using the  $S$  parameter [2] (i.e. the central area of the peak divided by the net peak area), which is a measure of the fraction of positrons annihilating with low momentum electrons. The H-induced lattice expansion was measured in the out-of-plane direction by XRD at HASYLAB (DESY) using synchrotron radiation with the wavelength  $\lambda = 1.12\text{ Å}$ . The TEM studies were performed with a Philips CM300SuperTWIN microscope operating at 300 kV. Thin foils for cross-sectional TEM were produced by conventional preparation using Gatan precision ion polishing system (PIPS).

\* Corresponding author. Tel.: +420 221912788; fax: +420 221912567.

E-mail address: jcizek@mbox.troja.mff.cuni.cz (J. Cizek).

### 3. Results and discussion

The TEM observations of the virgin films sputtered at room temperature revealed “column-like” elongated grains (width  $\approx 50$  nm). In the film’s cross-section the columns are divided horizontally into two “generations” of sub-columns with a height being approximately the half of the film thickness [4]. The “first generation” sub-columns are situated close to the Si substrate, while the “second generation” sub-columns grow on the top of the “first generation”. The nanocrystalline films exhibit a strong (1 1 0) texture, i.e. most grains are oriented so that the {1 1 0} planes are parallel with the substrate. On the other hand, the lateral orientation of the grains in the substrate plane is completely random. The diffraction profile of the (1 1 0) Nb reflection measured on the nanocrystalline virgin film is plotted in Fig. 1A, right part. The asymmetric shape of the profile indicates that it is a superposition of two contributions from the Nb layer with slightly different inter-planar spacing; see Ref. [4] for details. Taking into account the TEM observations, it indicates that the inter-planar spacing,  $d_{110}$ , of the {1 1 0} planes in the “first generation” and in the “second generation” sub-columns differ. It should be mentioned that the corresponding inter-planar spacing in bulk Nb is  $d_{110} = 2.3338$  Å [5] (the dashed line in Fig. 1A). Thus, it is clear that the out-of-plane  $d_{110}$  lattice spacing in both generations of the sub-columns are significantly larger than in bulk Nb. Moreover, we have found that  $d_{110}$  decreases with increasing tilting angle  $\psi$ . Such experimental findings can be explained by compressive stresses in the in-plane direction caused by bonding to the Si substrate. The “first generation” sub-columns are subjected to the highest compressive in-plane stresses because they are attached directly to the Si substrate. The magnitude of the compressive stress decreases with the distance from the interface with substrate. Thus, the “second generation” sub-columns situated on the top of the “first generation” exhibit more relaxed structure because they feel smaller in-plane stresses.

The diffraction profile for the epitaxial film (Fig. 1A, left part) is substantially narrower and can be well fitted by a single reflection. The  $d_{110}$  value for the epitaxial film lays close to

that for bulk Nb. It is due to: (i) the sapphire substrate, which is known to exhibit a good match with Nb lattice [6] and (ii) a high sputtering temperature, which enables a relaxation of the film layers. The thermal stresses during cooling of the film can be neglected because sapphire and Nb exhibit nearly identical thermal expansion coefficients [7].

The lattice expansion for the nanocrystalline and the epitaxial film is plotted in Fig. 1B as a function of H concentration,  $x_H$ . One can see that the out-of-plane lattice constant exhibits approximately linear increase with  $x_H$  in the  $\alpha$ -phase field. When the hydride-phase (Nb-H) is formed, additional peaks corresponding to its orthorhombic structure appear in the XRD spectra. The positions of the phase boundaries are shown by dashed and solid lines for the nanocrystalline and the epitaxial films, respectively. The epitaxial film undergoes phase transitions at similar H concentrations as bulk Nb. On the other hand, the nanocrystalline film exhibits roughly four times larger H solubility in the  $\alpha$ -phase, and the two-phase field is narrower compared to bulk Nb. The extended H solubility in the nanocrystalline films is likely due to the nanocrystalline grain size. It leads to a significant volume fraction of grain boundaries (GBs) which can accumulate more H atoms. Note that an enhanced H solubility in thin Nb films has been already reported in Ref. [8].

The dependence of the  $S$  parameter on the positron energy  $E$  for the virgin nanocrystalline and epitaxial film, respectively, is plotted in Fig. 2A and B. The  $S$  parameter was normalized to that for a defect-free bulk Nb. A drop of the  $S$  parameter at low energies is due to positron annihilations inside the Pd cap. The increasing fraction of positrons annihilating inside the Nb layer is reflected by an increase of the  $S$  parameter starting from  $E \approx 1$  keV. In the interval from 4 to 22 keV positrons annihilate mainly inside the Nb layer. Eventually, at high energies  $E > 22$  keV some positrons penetrate into the substrate which leads to a further change of the  $S$  parameter. In case of the Si substrate, the  $S$  parameter increases while for the sapphire substrate it becomes lower. One can see that the  $S$  parameter in the Nb layer in both films is significantly higher than 1. This indicates that the Nb layer contains defects. The nanocrystalline film exhibits remarkably higher  $S$  parameter values in the Nb layer than the

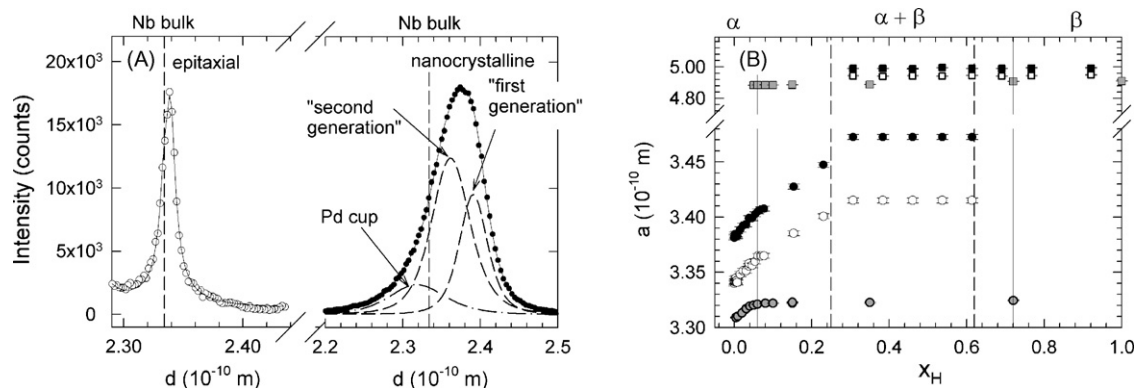


Fig. 1. (A) XRD diffraction profiles for the virgin films: open circles, epitaxial film; full circles, nanocrystalline film. Fit of the experimental points is plotted by the solid lines, while the dashed curves show the individual reflections which contribute to the profile. The distance between the {1 1 0} planes in bulk Nb is indicated by the dashed vertical lines. (B) The dependence of the lattice constant  $a$  on H concentration  $x_H$ . Nanocrystalline film:  $\alpha$ -phase, “first generation” (full circles),  $\alpha$ -phase, “second generation” (open circles),  $\beta$ -phase, “first generation” (full squares),  $\beta$ -phase, “second generation” (open squares); epitaxial film: the  $\alpha$ -phase (gray circles),  $\beta$ -phase (gray squares). Positions of the phase boundaries for the epitaxial and the nanocrystalline film, respectively, are indicated by solid and dashed vertical lines.

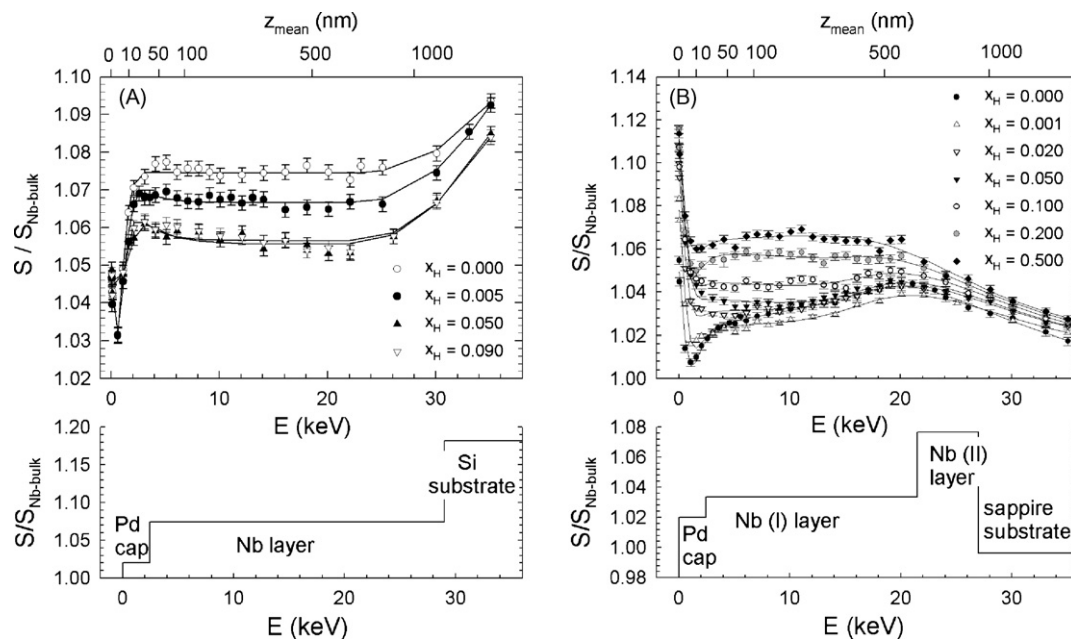


Fig. 2. *Upper panel*: Selected  $S(E)$  curves for the virgin film and the film loaded to various H concentrations: (A) nanocrystalline film, (B) epitaxial film. Fits of the experimental points are plotted by the solid lines. The mean positron penetration depth is shown in the upper  $x$ -axis. *Lower panel*: A schematic plot of the layers used to model the film. The height of each layer box equals to the  $S$  parameter of the layer in the virgin film.

epitaxial film. The nanocrystalline grain size leads to a significant volume fraction of GBs with vacancy-like open-volume defects. As a consequence, almost all positrons are trapped in these defects at GBs. Texture measurements showed that the epitaxial film is either a single crystal or consists of only a few grains with a weak miss-orientation. Thus, the volume fraction of GBs in the epitaxial film is negligible. However, it is known that the epitaxial Nb films contain misfit dislocations, which accommodate the lattice mismatch with the substrate. The misfit dislocation lines are situated either directly at the interface with the substrate or in a certain distance (stand-off) from the interface [6]. In addition, there is often a dislocation network expanded into the film which compensates the components of the misfit dislocation Burgers vectors which do not contribute to a relaxation of the lattice strain [9]. Thus, there is a defect-rich layer close to the substrate which should exhibit a larger  $S$  parameter than the remaining Nb layer. Indeed, one can see in Fig. 2B that the  $S$  parameter for the Nb layer is not constant for the epitaxial film, but increases with the depth. It testifies that the epitaxial film consists of a Nb layer (I) with a low defect density and a defected Nb layer (II) adjacent to the substrate with a high density of misfit dislocations.

The  $S$  parameter measured using positrons with certain energy  $E$  in a system consisting of  $N$  layers can be expressed as a superposition of the  $S$  parameters characteristic for each layer

$$S(E) = S_0 f_0(E) + S_1 f_1(E) + \dots + S_N f_N(E), \quad (1)$$

where  $S_0$  denotes the  $S$  parameter of positrons annihilated at the surface and  $S_i$  is the  $S$  parameter for the  $i$ th layer. The  $S$  parameters  $S_0$  and  $S_i$  ( $i=1, \dots, N$ ) are internal character-

istics of the surface and the  $i$ th layer, respectively. They are determined by the electron density and the concentration of defects in the corresponding layer and are independent on the positron energy. The fraction of positrons annihilating at the surface and inside the  $i$ th layer, respectively, is denoted  $f_0$  and  $f_i$ . Obviously  $f_0 + f_1 + \dots + f_N = 1$ . Higher positron energy leads to higher positron implantation depth and also wider positron implantation profile. In addition, thermalized positrons can diffuse between the adjacent layers. Thus, the fractions  $f_0, f_i$  depend on the positron energy and also on the positron diffusion length in each layer. The  $S$  parameter measured at certain energy  $E$  is given by the Eq. (1), i.e. it is a weighted average of the  $S$  parameters of the various layers where positrons with such energy annihilate. Fit of the experimental  $S(E)$  curves requires, therefore, to consider positron implantation profile and to solve positron diffusion equation for a layered system. In this work, we employed the VEPFIT software package [10], which uses the Makhovian positron implantation profile and solves numerically the positron diffusion equation. Detailed description of the fitting procedure can be found in Ref. [10]. From fit of the  $S(E)$  curves we obtained the  $S$  parameters characteristic for the layers considered in the model of the studied films, corresponding positron diffusion lengths, and positions of boundaries between the layers. In order to reduce the number of the fitted parameters we fixed the positron diffusion lengths for the substrates and the Pd cap at the values obtained from SPIS measurements of bare substrates and a Pd film sputtered under the same conditions as the Pd cap. In addition, we fixed the film thickness known from the TEM measurements. In case of the nanocrystalline films, we considered a three-layer model: 1-Pd cap, 2-Nb layer, 3-Si substrate. However, the three-layer model is inadequate for the epitaxial films because of the additional defected layer

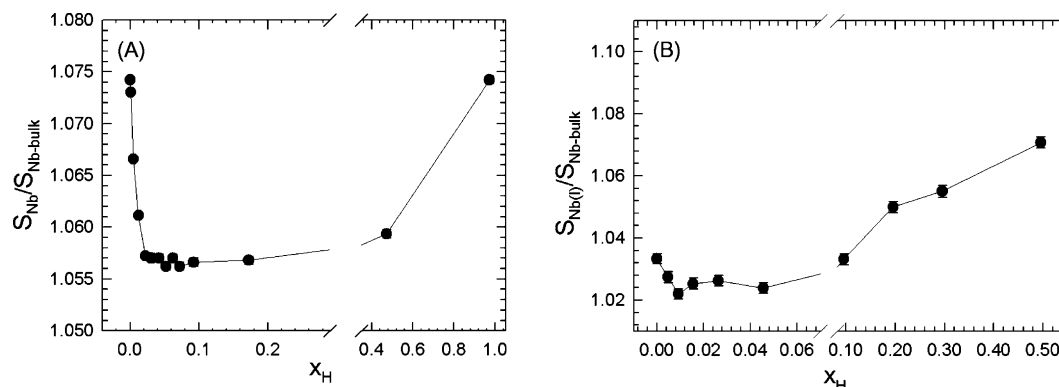


Fig. 3. Dependence of the  $S$  parameter obtained from fits of the  $S(E)$  curves on H concentration: (A) Nb layer—nanocrystalline film, (B) Nb(I) layer—epitaxial film.

with misfit dislocations adjacent to the substrate. It was found that the epitaxial films could be well fitted using a four-layer model: 1-Pd cap, 2-Nb(I) layer with lower density of defects, 3-Nb(II) layer with a high density of misfit dislocations, and four-sapphire substrate. The layer models of the studied films are shown schematically in Fig. 2A and B (lower panel). The fits of the experimental data are shown by solid lines in Fig. 2A and B. From the fit, we obtained the thickness of the defected layer Nb(II) adjacent to the substrate to be  $(100 \pm 20)$  nm.

The selected  $S(E)$  curves for H-loaded nanocrystalline and epitaxial films are plotted in Fig. 2A and B as well. The  $S$  parameter for the Nb layer,  $S_{\text{Nb}}$ , and the Nb(I) layer,  $S_{\text{Nb(I)}}$ , for the nanocrystalline and the epitaxial film, respectively, as they were obtained from fits of the  $S(E)$  curves are plotted in Fig. 3A and B as a function of H concentration  $x_{\text{H}}$ . One can see that the  $S$  parameter for the Nb layer is lowered in the films loaded at low H concentrations. It indicates that similarly to positrons also H is trapped at the open-volume defects, namely at GBs in the nanocrystalline films, and at the misfit dislocations in the epitaxial film. The presence of H bound to such a defect causes an increase of the local electron density, which leads to a decrease of positron localization and, thereby, to a decrease of the  $S$  parameter. The relative decrease of the  $S$  parameter in both films is approximately 2%. However, the  $S$  parameter values in the  $\alpha$ -phase field are lower in the epitaxial film indicating that there is certain fraction of positrons annihilating from the free-state. The decrease of the  $S$  parameter caused by H trapping at defects existing already in the virgin films is finished at  $x_{\text{H}} \approx 0.02$  and  $0.01$  in the nanocrystalline and the epitaxial film, respectively. A lower defect density in the epitaxial film causes that all the available defects are filled with H at lower  $x_{\text{H}}$ . At higher H concentrations, the  $S$  parameter reaches a plateau-like value suggesting that all the available open-volume traps are already filled with H and the local H concentration in the vicinity of defects reaches a steady state value. It should be mentioned that Fukai et al. found an extraordinary high number of vacancies is introduced by high-pressure H gas loading at high temperature [11]. Using PAS we found that vacancies surrounded by four H atoms are created in bulk Nb also by electrochemical H loading at room temperature [12]. The H-induced vacancies are introduced at low H concentrations  $x_{\text{H}} < 0.03$  and their concentration approaches  $3 \times 10^{-5} \text{ atom}^{-1}$  [12]. The SPIS

studies of the H-loaded bulk Nb performed in Ref. [12] showed that such concentration of the H-induced vacancies causes an increase of the  $S$  parameter by  $\approx 1.5\%$ . We expect the similarly to the bulk Nb samples, the H-induced vacancies surrounded by four H atoms are created in the Nb thin films as well. However, an important difference between the bulk Nb samples studied in [12] and the thin films consists in the fact that the films contain a significant concentration of defects already in the virgin state. The Nb(I) layer in the virgin epitaxial film exhibits the  $S$  parameter, which is by  $\approx 3.5\%$  higher than that for the bulk Nb. It testifies that defect density in this layer is higher or at least comparable with the concentration of the H-induced vacancies. The defect density in the nanocrystalline Nb layer is even much higher. There are two processes acting against each other in the films H-loaded in the  $\alpha$ -phase field: (i) hydrogen trapping at defects, and (ii) formation of the H-induced vacancy-4H complexes. The process (i) causes a decrease of the  $S$  parameter, while the process (ii) leads to an increase in  $S$ . Virtually all positrons in the nanocrystalline film are trapped at defects (saturated trapping). An addition of defects of similar kind cannot, therefore, change the  $S$  parameter. Thus, although the H-induced vacancies are formed, they do not cause an increase of the  $S$  parameter. On the other hand, the epitaxial film exhibits still a certain fraction of free positrons. Indeed, one can see in Fig. 3B that there is a slight increase of the  $S$  parameter for the Nb layer at  $0.01 < x_{\text{H}} < 0.03$ . This increase is most probably due to the H-induced vacancy-4H complexes.

The formation of the hydride-phase particles occurs at  $x_{\text{H}}$  larger than 0.25 and 0.06 for the nanocrystalline and the epitaxial films, respectively. It is known that dislocation loops may be emitted by growing hydride particles. In addition, positrons can be trapped at misfit defects at the interface between a hydride-phase precipitate and the matrix. Indeed, as one can see in Fig. 3A and B, the  $S$  parameter exhibits an increase when the hydride-phase precipitates. Thus, we can conclude that the formation of the hydride-phase particles leads to an introduction of new open-volume defects.

#### 4. Conclusions

In the present work, we performed defect studies of H-loaded nanocrystalline and epitaxial Nb film with a thickness of  $1.1 \mu\text{m}$ .

The films exhibit a high density of defects already in the virgin state. It was found that the H solubility in the  $\alpha$ -phase in the nanocrystalline film is four times larger than in bulk Nb. The epitaxial film contains a defected layer with a high density of misfit dislocations situated close to the substrate, while the remaining film layer contains substantially lower concentration of defects. The SPIS measurements revealed that H is trapped at open-volume defects at GBs and at the misfit dislocations in the nanocrystalline and epitaxial films, respectively, which is seen by a decrease of the  $S$  parameter. Formation of the hydride-phase particles introduces new defects into the films.

### Acknowledgements

Financial support from the Czech Science Foundation (project No. 202/05/0074), the Ministry of Education of The Czech Republic (projects No. MS 0021620834), the INTAS (project INTAS-05-1000005-7672) the HASYLAB and the Alexander von Humboldt Foundation is highly acknowledged.

### References

- [1] R. Kirchheim, *Prog. Mater. Sci.* 32 (1988) 261–325.
- [2] P. Hautojärvi, C. Corbel, in: A. Dupasquier, A.P. Mills (Eds.), *Proceedings of the International School of Physics “Enrico Fermi”, Course CXXXV*, IOS Press, Varena, 1995, pp. 491–562.
- [3] W. Anwand, H.-R. Kissener, G. Brauer, *Acta Phys. Polonica A* 88 (1995) 7–11.
- [4] J. Čížek, I. Procházka, G. Brauer, W. Anwand, A. Mücklich, R. Kirchheim, A. Pundt, C. Bähz, M. Knapp, *Appl. Surf. Sci.* 252 (2006) 3237–3244.
- [5] ICDD (International Centrum for Diffraction Data) Powder diffraction Pattern Database PDF-2.
- [6] A.R. Wildes, J. Mayer, K. Theis-Bröhl, *Thin Solid Films* 401 (2001) 7–34.
- [7] J.B. Wachtmann, T.G. Scuderi, G.W. Cleek, *J. Am. Ceram. Soc.* 45 (1962) 319.
- [8] S. Moehlecke, C.F. Majkrzak, M. Strongin, *Phys. Rev. B* 31 (1985) 6804–6806.
- [9] D.M. Tricker, W.M. Stobbs, *Philos. Mag. A* 71 (1995) 1051.
- [10] A. van Veen, H. Schut, M. Clement, J. de Nijs, A. Kruseman, M. Ijma, *Appl. Surf. Sci.* 85 (1995) 216–221.
- [11] Y. Fukai, *J. Alloys Compd.* 356–357 (2003) 263–269.
- [12] J. Cizek, I. Prochazka, F. Becvar, R. Kuzel, M. Cieslar, G. Brauer, W. Anwand, R. Kirchheim, A. Pundt, *Phys. Rev. B* 69 (2004) 224106.